# Synthesis, Structural and Spectroscopic Characterization of Four [($\eta^6$-PAH)Cr(CO)$_3$] Complexes (PAH = Pyrene, Perylene, Chrysene, 1,2-Benzanthracene)

**Aldo Arrais,[a] Eliano Diana,[b] Giuliana Gervasio,*[b] Roberto Gobetto,[b] Domenica Marabello,[b] and Pier Luigi Stanghellini*[a]**

**Keywords:** Macrocyclic ligands / Chromium / X-ray diffraction / NMR spectroscopy / Vibrational spectroscopy / DFT calculations

The thermal reaction of hexacarbonylchromium with the polycyclic aromatic hydrocarbons (PAHs) pyrene, perylene, chrysene and 1,2-benzanthracene has afforded four organometallic complexes of the type [($\eta^6$-PAH)Cr(CO)$_3$], whose unprecedented structures were obtained by single-crystal X-ray analysis. The topology of the coordination of the Cr(CO)$_3$ fragment and its asymmetry with respect to the coordinating ring may depend on the opportunity to maintain the maximum aromaticity of the complexed ligand. DFT calculations, $^1$H NMR, FT-IR and Raman spectroscopy have been used to elucidate the type of interaction between the PAH ligand and the carbonylmetal moiety, giving insight into the ligand-to-metal donor capacity and the intra- and intermolecular interactions.


## Introduction

Polycyclic aromatic hydrocarbons (PAHs) have long been investigated in diverse fields of research, ranging from astrophysics[1] to molecular biology.[2] [(PAH)Cr(CO)$_3$] complexes are efficient organometallic precursors for the organic synthesis of PAH derivatives by selective nucleophilic attack on the metallated ring.[3] Some can also exhibit chirality, which is useful in stereochemical reactions for drug design as, in vivo, PAHs have multiple well-documented carcinogenic effects.[4]

In the solid state, PAHs often assume a layered architecture;[5] which suggests that they have potential as synthons in crystal engineering and in preparing advanced molecular solids.[6] Actually, the large delocalization of π-electron density allows the formation of complexes where intermolecular coupling ranges from weak interactions to the formation of charge-transfer complexes.[7] Alongside the well-known adducts of PAHs with classical electron-transfer organic counterparts, such as tetracyanoethylene (TCNE),[8] tetracyanoquinodimethane (TCNQ)[9] and 2,3-dichloro-5,6-dicyano-*p*-benzoquinone (DDQ),[10] more recently a few organometallic complexes have appeared, such as the ferrocene−pyrene system.[11] Two promising examples of [($\eta^6$-arene)Cr(CO)$_3$]- and [($\eta^6$-PAH)Cr(CO)$_3$]-type structures have been reported, i.e. the non-centrosymmetrical complex (benzene)Cr(CO)$_3$/thiourea[12] and the complex (phenanthrene)Cr(CO)$_3$/1,3,5-trinitrobenzene.[13] Interest in the latter derivatives is strengthened by the presence of the metal atom, which can tune the electronic properties of the adducts and allow the isolation of materials displaying useful magnetic and optical properties.[14,15]

Carbonyl(PAH)chromium derivatives also tend to maintain, in the solid state, a face-to-face packing of the aromatic rings, and they can provide carbonyl groups that can interact through weak intermolecular interactions such as the C−H···O hydrogen bond, which is crucial in the design of suitable molecular building blocks in crystal engineering.[16]

From these perspectives, we attempted to synthesise [($\eta^6$-PAH)Cr(CO)$_3$] complexes, including large polycyclic aromatic compounds, focusing upon four important PAH frameworks: pyrene, perylene, chrysene and 1,2-benzanthracene. There are few reports of such large complexed ligands,[17] the main published derivatives concerning instead the homologues of [($\eta^6$-benzene)Cr(CO)$_3$].[18−22] In fact, only four examples of [($\eta^6$-PAH)Cr(CO)$_3$] complexes, where PAHs are unsubstituted naphthalene,[23] an-

[a] Dipartimento di Scienze e Tecnologie avanzate, Università del Piemonte Orientale,
Corso T. Borsalino 54, 13100 Alessandria, Italy
Fax: (internat.) + 39-0131-287416
E-mail: pierluigi.stanghellini@unito.it
pierluigi.stanghellini@unipmn.it
[b] Dipartimento di Chimica I. F. M., Università di Torino,
Via P. Giuria 7, 10125 Torino, Italy
Fax: (internat.) + 39-011-6707855
E-mail: giuliana.gervasio@unito.it
Supporting information for this article is available on the WWW under http://www.eurjic.org or from the author.

thracene,[24] phenanthrene[25] and triphenylene,[26] have been structurally determined.[27] For the former large PAH structures, however, a few metal coordination studies have been reported, with Ru,[28−31] Fe,[32,33] Mo[33,34] and Ti[35] as the $\eta^6$-bonded metal atoms. The PAH ligands used in the present work are illustrated in Scheme 1.

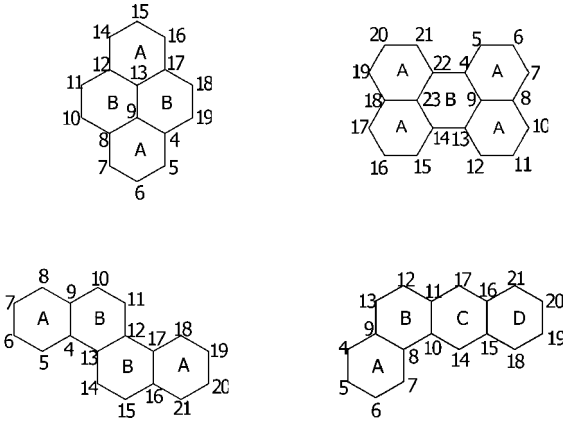

Scheme 1. Structure of the polycyclic aromatic hydrocarbon ligands pyrene, perylene, chrysene and 1,2-benzanthracene (the C atom numbering starts from C-4, as C-1, C-2 and C-3 always refer to carbonyl carbon atoms

## Results and Discussion

### Structure of the Complexes

(Pyrene)-, (perylene)-, (chrysene)- and (1,2-benzanthracene)tricarbonylchromium complexes (Figures 1−4) all coordinate the $Cr(CO)_3$ group on the face of a peripheral ring, with the metal atom ca. 1.74 Å from the ring centroid. The carbon atoms of the four ligands lie in a plane with a mean deviation from planarity of 0.021 (**1**), 0.028 (**2**), 0.029 (**3**) and 0.034 Å (**4**). The carbonyl groups lie between a staggered and an eclipsed orientation with respect to the carbon atoms of the coordinated ring. The plane formed by the three oxygen atoms is parallel to the plane of the coordinated ring; however, the chromium atom is not symmetrically linked to the six atoms of the aromatic ring, as occurs,

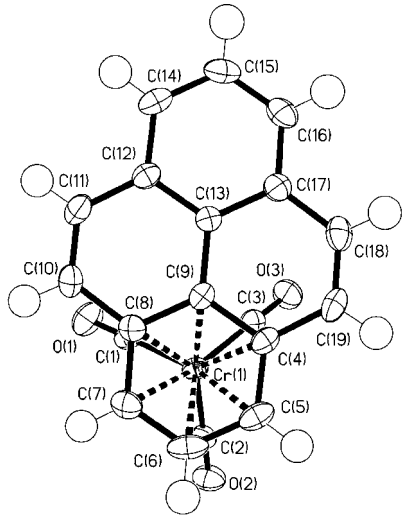


Figure 1. ORTEP plot of the complex [($\eta^6$-pyrene)$Cr(CO)_3$] (**1**) (30% probability for the thermal ellipsoids) with the atom labeling

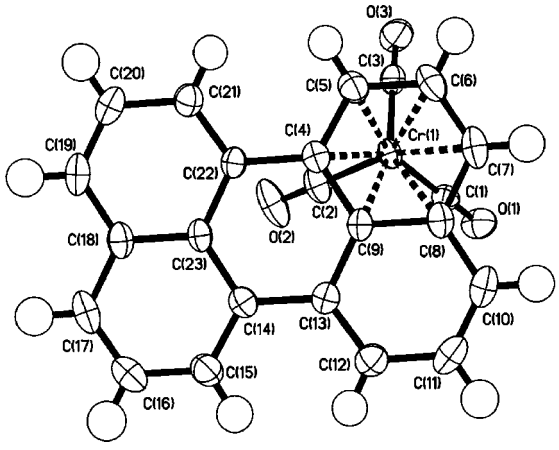


Figure 2. ORTEP plot of [($\eta^6$-perylene)$Cr(CO)_3$] (**2**) (30% probability for the thermal ellipsoids) with the atom labeling

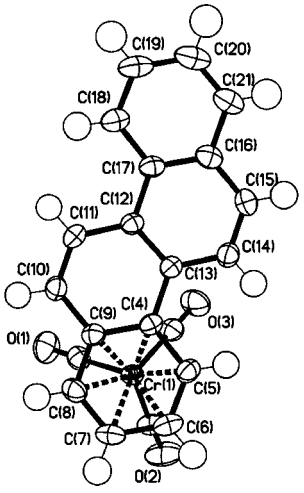


Figure 3. ORTEP plot of [($\eta^6$-chrysene)$Cr(CO)_3$] (**3**) (30% probability for the thermal ellipsoids) with the atom labeling

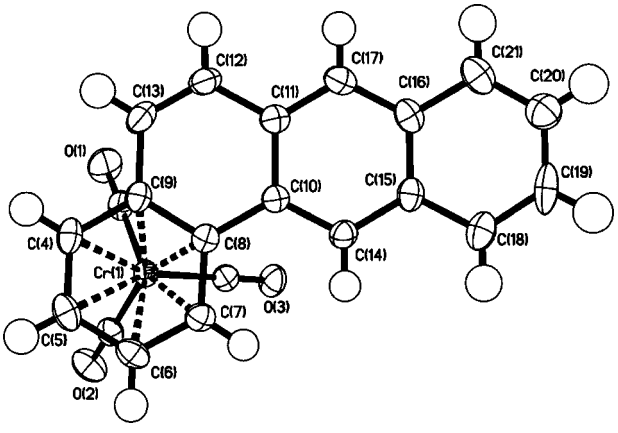


Figure 4. ORTEP plot of complex [($\eta^6$-benzanthracene)$Cr(CO)_3$] (**4**) (30% probability for the thermal ellipsoids) with the atom labeling

  

Table 1. Selected bond lengths [Å] and angles [°] for complexes **1**−**4**

| Complex | **1** | **2** | **3** | **4** |
|---|---|---|---|---|
| Cr(1)−C(1) | 1.831(3) | 1.828(3) | 1.833(3) | 1.831(2) |
| Cr(1)−C(2) | 1.812(3) | 1.821(3) | 1.822(3) | 1.834(3) |
| Cr(1)−C(3) | 1.830(3) | 1.832(3) | 1.836(3) | 1.834(2) |
| Cr(1)−C(4) | 2.268(3) | 2.241(2) | 2.273(3) | 2.210(2) |
| Cr(1)−C(5) | 2.219(3) | 2.210(3) | 2.217(3) | 2.209(2) |
| Cr(1)−C(6) | 2.192(3) | 2.200(3) | 2.224(3) | 2.206(2) |
| Cr(1)−C(7) | 2.214(3) | 2.221(3) | 2.217(3) | 2.204(2) |
| Cr(1)−C(8) | 2.272(3) | 2.294(3) | 2.212(3) | 2.271(2) |
| Cr(1)−C(9) | 2.282(3) | 2.288(2) | 2.280(3) | 2.265(2) |
| C(1)−O(1) | 1.142(3) | 1.156(3) | 1.163(3) | 1.154(2) |
| C(2)−O(2) | 1.154(3) | 1.157(3) | 1.147(3) | 1.152(3) |
| C(3)−O(3) | 1.148(3) | 1.150(3) | 1.143(3) | 1.150(2) |
| C(4)−C(5) | 1.403(3) | 1.396(3) | 1.436(3) | 1.377(3) |
| C(4)−C(9) | 1.431(3) | 1.437(3) | 1.415(3) | 1.428(3) |
| C(5)−C(6) | 1.393(4) | 1.391(4) | 1.387(3) | 1.407(3) |
| C(6)−C(7) | 1.375(3) | 1.374(4) | 1.400(4) | 1.384(3) |
| C(7)−C(8) | 1.419(3) | 1.422(4) | 1.381(4) | 1.425(3) |
| C(8)−C(9) | 1.413(3) | 1.429(3) | 1.419(3) | 1.421(3) |
| Other C−C bonds | 1.324−1.439(3) | 1.343−1.471(3) | 1.332−1.446(3) | 1.338−1.458(3) |
| C(1)−Cr(1)−C(2) | 89.54(11) | 89.44(12) | 89.67(13) | 88.45(10) |
| C(1)−Cr(1)−C(3) | 89.20(11) | 88.97(12) | 88.76(13) | 89.43(10) |
| C(2)−Cr(1)−C(3) | 88.87(12) | 89.30(13) | 88.12(13) | 89.15(10) |
| O(1)−C(1)−Cr(1) | 178.5(3) | 179.5(3) | 178.4(2) | 179.0(2) |
| O(2)−C(2)−Cr(1) | 179.3(3) | 177.6(3) | 178.1(3) | 178.8(2) |
| O(3)−C(3)−Cr(1) | 179.0(3) | 178.4(3) | 179.5(3) | 179.7(2) |

for example, in [{$C_6(CH_3)_6$}Cr(CO)$_3$].[36] The chromium atom is significantly farther from the carbon atoms connected to the condensed rings than the remaining Cr−$C_{ring}$ distances (Table 1).

Coordination of a metal atom to an aromatic ring sometimes modifies the structure of the ring, typically by expansion of the ring, the loss of planarity of the ring and alternation of long and short C−C bonds.[37] In our case, the ligands are planar. Regular alternating of short/long C−C bonds of the coordinated ring may be observed in complexes **3** and **4** only where the coordinated ring is condensed to another ring.[38−41] In all complexes, however, the bonds adjacent to the coordinated rings are significantly long and therefore have a minor double-bond character. Further, C(10)−C(11) [1.327(3) Å] and C(18)−C(19) [1.324(3) Å] bonds in **1**, C(10)−C(11) [1.343(4) Å] and C(12)−C(13) [1.364(3) Å] bonds in **2**, C(10)−C(11) [1.332(3) Å] bond in **3** and C(12)−C(13) [1.326(3) Å] bond in **4** all show values corresponding to a double bond. Also, a set of short C−C bonds is located in the ligand on the opposite side with respect to the metal atom. We are confident of the accuracy of these values, even though the structural data of the complexes were collected at room temperature: in fact the estimated standard deviations (e.s.d.) of the C−C bond lengths are 0.003−0.004 Å.[42]

Considering the structural data, as expected there is no more than a negligible change in the PAH structures, owing to the very hard deformability of the fused rings. Variations of some structural parameters concerning the metal fragment and the relationship between the PAH and this fragment are expected to be more significant, such as (i) the average Cr−$C_{CO}$ distance in the coordinated Cr(CO)$_3$ fragment and (ii) the distance between the chromium atom and the arene centroid. Table 2 collects these data, together with those of some other selected complexes with either greatly electron-releasing (diethylaminobenzene and hexamethylbenzene)[43] or electron-withdrawing (hexachlorobenzene)[44] arenes. Also included are some well-known [(PAH)Cr(CO)$_3$] complexes, together with [Cr(CO)$_6$] because of the exceptional electronic withdrawal of the (CO)$_3$ unit. The clear variation shown in Cr−$C_{CO}$ is typical of an L−M−CO unit and of the well-known relationship between charge transfer and bond length. Thus, electron transfer from arene to Cr causes a significant shortening of the Cr−CO bond and vice versa a charge demand elongates this bond length. Accordingly, diethylaminobenzene shows the shortest distance[43] and hexachlorobenzene[44] {and, of course, [Cr(CO)$_6$]} the longest.[45] ν(CO) is another indirect, but sensible, parameter by which to measure this charge transfer.[46] Accordingly, the hexamethylbenzene complex shows the lowest and the hexachlorobenzene the highest value. The PAH ligands lie in between, showing a medium donating character; among them, pyrene is the best donating ligand, whereas perylene is the worst. The Cr−centroid distances [point (ii) above] are less significant in classifying charge-transfer effects, because arenes with substantial differences in donor−acceptor properties sometimes exhibit similar M−arene distances. Nevertheless, a long Cr−CO distance roughly corresponds to a short Cr−ring distance.

### Bonding

The topology of the coordination of the Cr(CO)$_3$ fragment on the PAH ring is significant. Even if a statistical effect could be invoked for perylene, for all the other ligands

  

Table 2. Structural and spectroscopic parameters of selected [($\eta^6$-arene)$Cr(CO)_3$] complexes

| Ligand | $Cr-C_{arene}$ [Å][a] | $Cr-C_{CO}$ [Å] | $Cr-C_{ring\ centroid}$ [Å] | $\nu_{CO}$ ($A_1$) [$cm^{-1}$] [60] | Ref. |
|---|---|---|---|---|---|
| $(CO)_3$ | | 1.915(2) 74K | | 1987 | [61] |
| Hexachlorobenzene | 2.200(5) | 1.879(5) av. | 1.680(5) | 2009 | [62] |
| Benzene | 2.220−2.240(2) (78 K, neutr.) | 1.842(2) av. | 1.726(2) | 1974 | [43] |
| Naphthalene | 2.20 | 1.82 av. | | 1977 | [21] |
| (triclinic form) | 2.32 | | | | |
| Anthracene | 2.218(9) | 1.82(1) av. | 1.76(1) | 1978 | [22] |
| | 2.332(8) | | | | |
| Phenanthrene | 2.210(5) | 1.834(6) av. | | 1980 | [24] |
| (monoclinic form) | 2.283(5) | | | | |
| Phenanthrene | 2.209(4) | 1.828−1.857(5) | 1.733(5) | 1980 | [23] |
| (orthorhombic form) | 2.289(4) | | | | |
| Pyrene (**1**) | 2.208(3) | 1.812−1.831(3) | 1.746(3) | 1959 | this work |
| | 2.274(3) | | | | |
| Perylene (**2**) | 2.220(3) | 1.821−1.832(3) | 1.745(3) | 1968 | this work |
| | 2.274(3) | | | | |
| Chrysene (**3**) | 2.217(3) | 1.822−1.836(3) | 1.740(3) | 1965 | this work |
| | 2.277(3) | | | | |
| Benzanthracene (**4**) | 2.207(2) | 1.832(3) av. | 1.727(2) | 1966 | this work |
| | 2.268(2) | | | | |
| Triphenylene | 2.204(3) | 1.833(3) av. | 1.720(3) | 1990 (KBr) | [25] |
| | 2.258(3) | | | | |
| Hexamethylbenzene | 2.241(3) | 1.836(3) av. | 1.730(3) | 1948 | [36] |
| 1,2,3-Trimethoxybenzene | 2.224(2) | 1.830−1.845(2) | 1.755(2) | 1963 | [63] |
| | 2.281(2) | | | | |
| Diethylaminobenzene | 2.185(2)−2.369(2) | 1.813(2)av. | 1.750(2) | 1954 | [63] |

[a] The first value is the average Cr−C(ring-unsusbstituted) bond length, the second one is the average Cr−C(ring-junction) bond length.

the probability of the coordinating ring to bond the metal fragment is identical to that of any other ring types. The observed regioisomerism of the coordination could be explained by the different aromaticity between the free and the bonded PAH, which can be simply represented by the number of possible Kekulé covalent structures (KS).[47] In all cases KS decreases as a consequence of coordination. The real structure is that which, compared to the other possibilities, maintains the maximum aromaticity of the bonded ligand (Table 3). This simple approach agrees with the observed localized short and long C−C bond lengths found in the structures and also satisfactorily explains one of the most interesting stereochemical features of these complexes, that is the slipping of the $Cr(CO)_3$ fragment towards the unsubstituted carbon atoms of the arene ring and away from the ring junction carbon atoms.

Table 3. Number of the possible Kekulè structures (KS) of free and coordinated PAH ligands

| Complex | **1** | **2** | **3** | **4** |
|---|---|---|---|---|
| Coordinating ring[a] | A B | A B | A B | A B C D |
| Number of KS | 4 2 | 6 4 | 6 4 | 6 4 4 4 |
| Number of KS of the free ligand | 6 | 9 | 8 | 7 |
| A[b] | 1.5 | 1.5 | 1.3 | 1.2 |

[a] See Scheme 1. [b] Aromatic loss, i.e. the ratio between no. of KS of the free ligand with respect to the stable form of the coordinated ligand.

From another point of view, this agrees with the suggestion that, for non-symmetric aromatic rings, the metal atom should bind to the more electron-rich double bond.[48−49] The external C−C bonds have an overall double-bond character greater than that of the ring-junction C−C bond. Moreover, another effect can be present, which is a repulsion between the π-electron charge delocalized on the adjacent non-bonded rings and the negative charge induced on the Cr atom by the donation of the bonded ring. A closely related phenomenon has been evidenced in a series of [(substituted arene)$Cr(CO)_3$] complexes, where the electron repulsion tilts the arene substituents away from Cr.[21] If in the PAH ligand the adjacent ring can be viewed as a substituent of the bonded ring, as the overall structure is hardly deformable, it is the $Cr(CO)_3$ group that shifts towards the peripheral carbon atoms.[50]

To substantiate the previous simplified approach, a quantum mechanical calculation of the total energy has been performed.[51] The chosen model was complex **4**, which displays the highest number of possible regioisomers, named as the A, B, C and D complexes, according to the coordinating ring (Scheme 1). We made a single-point calculation on an idealized structure with the Cr atom perpendicular to the centre of the coordinating ring and the carbonyl groups in the staggered position with respect to the carbon atoms. For complex A, a calculation has also been carried out on the real structure: the difference is irrelevant. The B3LYP DFT method was used with a pseudopotential LANL2DZ basis set for the chromium atom and the 6-

  

31G(d, p) basis for the other atoms. Figure 5 shows both the total energy and of the Mulliken charge on the Cr atom. Complex A is clearly the most stable conformation, as predicted by simple KS counting. The charge on the Cr atom can be related to the DFT-Mulliken mean charge density in the rings of the free 1,2-benzanthracene, which is D (−0.194) < A (−0.0368) < B (0.0254) < C (0.0327). As the main contribution to the PAH−Cr bond is the electron donation PAH→Cr, the most stable configuration should be given by the Cr coordination to the ring with the highest electron density. The A ring is preferred to the D ring, probably because of the maintenance of the maximum aromatic stabilisation energy.

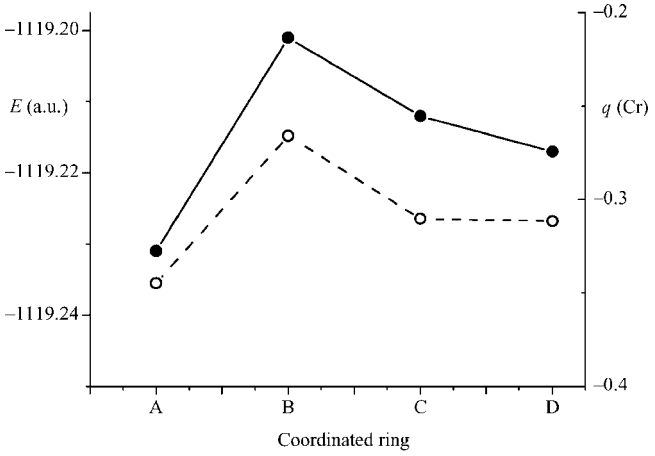


Figure 5. Total energy of the regioisomers of complex **4** (closed circles); Mulliken charge on the Cr atom (open circles)

Finally, the theoretical approach can be related to simple chemical properties of the complexes. For example, the linear PAHs, 1,2-benzanthracene in particular, whose aromaticity loss in the coordination is lower, are more stable and are obtained in better yield than the condensed PAHs.

### Vibrational Analysis

The vibrational pattern of the [(PAH)Cr(CO)$_3$] complexes can be roughly divided into three types of modes, those of the PAH ligand, those of the Cr(CO)$_3$ unit and those derived by the interaction between the two fragments. In a first approximation the coupling between these sets of modes is negligible;[52] thus, a close comparison with the spectra of the free ligand is of significant help in the assignment. As an example, Figures 6 and 7 show the infrared and the Raman spectra of complex **1**, together with those of the ligand. The modes of the Cr(CO)$_3$ unit are immediately evident, as a very strong band in the 2000−1800 cm$^{-1}$ region [ν(CO)] and in the 700−400 cm$^{-1}$ region [δ(Cr−CO) and ν(Cr−CO)]. More doubtful is the assignment of the PAH−Cr modes, which lie below 300 cm$^{-1}$ and are mixed with the ring deformation modes. Usually, only the PAH−Cr stretching can be assigned with some confidence to a medium-strong Raman band around 290 cm$^{-1}$. The remaining band pattern concerns the vibrations of the coordinated PAH ligand.

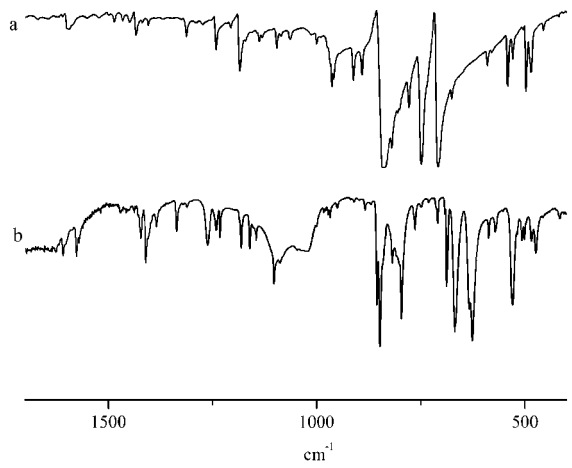


Figure 6. Solid-state infrared spectra in the 1600−400 cm$^{-1}$ region of pyrene (a), complex **1** (b)

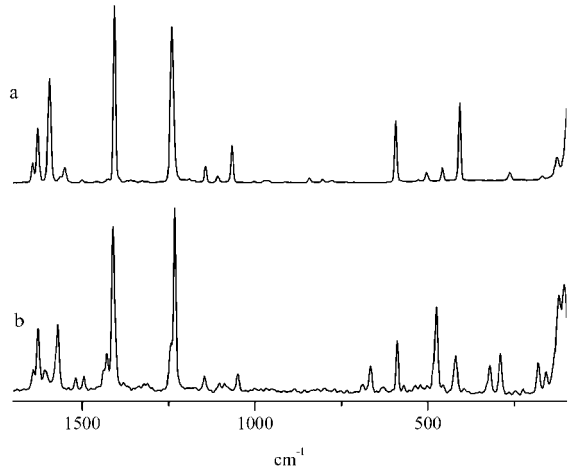


Figure 7. Solid-state Raman spectra in the 1600−200 cm$^{-1}$ region of pyrene (a) complex **1** (b)

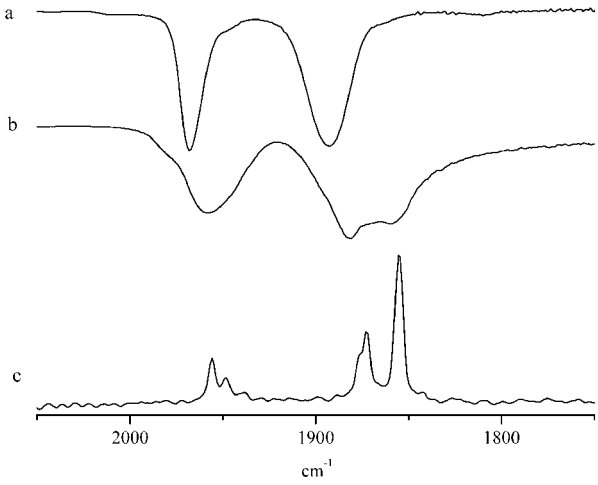


Figure 8. Spectra of complex **2** in the $\nu_{CO}$ region; (a): solution (toluene) infrared, (b): solid state infrared, (c): solid-state Raman

  

The infrared ν(CO) spectrum in aliphatic and aromatic hydrocarbon solutions shows the usual behavior of an $M(CO)_3$ group with a local $C_{3v}$ symmetry: a medium-strong high-frequency band ($A_1$) and a strong, broad (sometimes split) band at lower frequency (E). Both the IR and Raman spectral patterns in the solid state are more complex, because of the site and/or factor group effects, and are shifted to lower frequencies by 15−25 $cm^{-1}$, with respect to those in solution (Figure 8). This is clear spectroscopic evidence of what has been observed in the crystal packing, i.e. many C−H···O interactions.

The modes of the coordinated and uncoordinated aromatic ligand lie in typical fingerprint regions,[53] corresponding to C−H stretching (3200−3000 $cm^{-1}$), in-plane C−C stretching and C−H bending (1600−900 $cm^{-1}$), to out-of-plane C−H bending (900−700 $cm^{-1}$) and to out-of-plane C−C bending (below 500 $cm^{-1}$). Significant changes are evident in the ν(CH) region: the modes of the coordinated PAH move up with respect to those of the free PAH. The Raman spectra, which give rise to medium-strong bands, are clear in this respect (Figure 9). Separation of the CH vibrations of the bonded ring from those of the non-bonded ring is inapplicable. As DFT calculations on the free PAH show that the CH vibrators are strongly coupled, the pattern has to be considered as a whole.

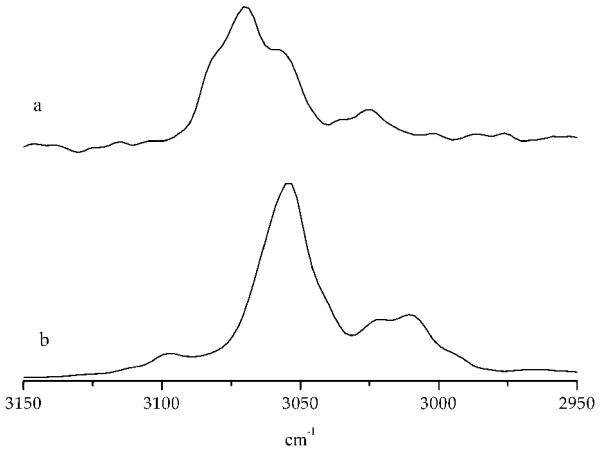


Figure 9. Solid-state Raman spectra of complex **1** (a), pyrene (b)

Even more interesting is the behavior of the γ(CH) modes, which are the most evident infrared fingerprint bands of the aromatic hydrocarbons, and are sensitive to the effect of metal coordination, usually reflected in an increase in the frequency.[52,54−56] For example, the IR spectrum of free pyrene shows two very strong bands at 838 and 748 $cm^{-1}$, easily assigned to the γ(CH) modes, which are clearly shifted to 855 and 796 $cm^{-1}$ in complex **1**. The average shift (ca. 40 $cm^{-1}$) is similar to that found for perylene and complex **2** (ca. 30 $cm^{-1}$), but is definitely smaller than for the couple benzene/(benzene)$Cr(CO)_3$ ($\Delta\tilde{\nu} \approx 120$ $cm^{-1}$).[56] The γ(CH) modes have been separated into small sub-sets, corresponding to the vibrations of groups of adjacent H atoms (quadruplet, triplet, doublet and hydrogen solo).[53] Here too, DFT calculations show that this distinction is too rough and unacceptable, as the vibration of the CH units are all coupled. So the contribution to a γ(CH) mode is given by the vibration of all the CH units, belonging both to coordinated and to uncoordinated rings, and it is reasonable to expect that the last ones can attenuate the coordination effect. It could be relevant that with the linear PAH (chrysene and 1,2-benzanthracene) the attenuating effect of the uncoordinated part of the ligand is significant, because $\Delta\tilde{\nu}$ is very small (3 and 2 $cm^{-1}$, respectively).[57]

Usually, both ν(CH) and γ(CH) frequencies increase as a consequence of metal coordination, an explanation for which must include the extended framework of hydrogen bonds. This is an important factor in the rise of γ(CH), as a bending vibration that pulls the H atoms away from the equilibrium position is rendered more difficult by C−H···O interactions. The comparison between the spectra in the solid state and in solution is clear: in the last case rather small increases occur.[58] Presumably, the metal−ring interaction could also contribute to the shift − similar to the contributions observed in metallocene complexes.[52]

Conversely, the hydrogen interaction is expected to decrease ν(CH), so that the observed increase may be due to a simultaneous phenomenon that reinforces the C−H bond, thereby increasing the frequency. The π-donation from ring to metal atom might stabilize the σ frame, and so increase the C−C and C−H bond strengths. Owing to the small mass of hydrogen, ν(CH) values are particularly susceptible to small modifications of the C−H bond.

The vibrational pattern may also give some insight into the donor−acceptor properties of the PAH ligands. Theoretical and experimental infrared spectra have been reported to show significant differences in the intensity of the spectral regions between PAH molecules and the corresponding $[PAH]^+$ ions.[53][59] In particular, the latter exhibit an enhanced intensity in the ν(CC) and δ(CH) regions and a decreased intensity in the ν(CH) and γ(CH) regions with respect to the corresponding neutral molecule. On this basis an estimate of the intensity ratio $IR = \{I[\nu(CC) + \delta(CH)]/I[\nu(CH) + \gamma(CH)]\}$ for both free and complexed PAH could give information on the variation of the charge on the PAH as a consequence of coordination. Indeed, *IR* increases significantly from free to coordinated PAH for both pyrene (0.73 to 1.63) and chrysene (0.48 to 1.20), suggesting that these ligands are good donors, where the other two PAHs, which show the opposite trend (perylene: from 1.10 to 0.68; 1,2-benzanthracene: from 1.1 to 0.37), are bad donors.

### NMR Analysis

VT $^1H$ NMR spectra can allow the assignment of the aromatic protons of the four complexes on the basis of simple chemical shift/scalar coupling considerations, double resonance measurements and 2D $^1H$-$^1H$ results.

In all cases, the coordination induces typical high-field shifts and a decrease of the scalar $^3J_{H,H}$ couplings. This upfield shift can be a combination of different effects such as partial sp rehybridization of the ring carbon atom, an increase in electron density on the aromatic ring, quenching of the ring current, or magnetic anisotropy of the

  

chromium−ligand bond, as previously discussed.[60−63] The maximum up-field shift due to interaction with the $Cr(CO)_3$ fragment ($\Delta\delta$) occurs for the inner protons belonging to the peripheral ring, which supports metal coordination ($\Delta\delta$ = 3.06, 2.27, 2.71 and 2.70 ppm for **1**−**4**, respectively). The other protons belonging to the coordinated ring show $\Delta\delta \approx$ 2 ppm, whereas the chemical shifts of the protons of the uncoordinated rings are very close to those corresponding to the free ligand ($\Delta\delta \approx 0.2-0.6$ ppm). Detailed data are reported in Table 1SI of the Supporting Information (see also the footnote on the first page of this article).

We also attempted to evaluate the possible migration of the $Cr(CO)_3$ fragment on the different aromatic rings. Thermally induced rearrangements have been previously detected in many π complexes, e.g. in monosubstituted [(naphthalene)$Cr(CO)_3$][64−66] and monosubstituted [(biphenyl)$Cr(CO)_3$][67] derivatives. Haptotropic rearrangements reportedly require substantial activation energies, except in the presence of a coordinating solvent.[68,69] We thus performed a $^1$H NMR study of complexes **1**−**4**. However, under our experimental conditions (from −100 to +80 °C, deuterated toluene solutions, presence of the free ligand), no line broadening of the $^1$H resonances was observed, ruling out a fast degenerate haptotropic shift. This is not so surprising if the large energy differences of the possible regioisomers are considered, as has been evaluated for complex **4** by DFT calculations. Spin saturation transfer experiments[70] were also performed with complex **2**, which shows no energy differences between the possible regioisomers. No decrease in the intensity of the aromatic resonances were observed at +80 °C under saturation of the protons 5, 6 and 7, ruling out any haptotropic motion.

## Experimental Section

**Reactants and Solvents:** Pyrene, perylene, chrysene and 1,2-benzanthracene (Aldrich), hexacarbonylchromium (Fluka) were commercial products and were used without further purification. SilicaGel60 was purchased from Merck. The solvents, *n*-heptane, petroleum benzin and toluene (Riedel), were dried with sodium and kept under $N_2$.

***Warning:*** *Chrysene and 1,2-benzanthracene are active carcinogenic agents. They must be handled using all possible safety precautions, avoiding any contact or exposure.*

**Synthesis of the Complexes:** The synthetic methods used for the four complexes are very similar. We report as an example the detailed synthesis of the pyrene complex; for the other complexes, basic data are given.

**(a) [(Pyrene)Cr(CO)$_3$] (1):** Pyrene (250 mg, 1.24 mmol) was dissolved in petroleum benzin (boiling range 100−140 °C; 40 mL) in a flask (250 mL) equipped with an inlet inert gas bubbler and a reflux condenser. An Hg outlet bubbler was used to prevent air entering during the reaction. A gentle flow of $N_2$ was maintained for a few minutes to purge air from the flask. Hexacarbonylchromium (1.25 g, 5.68 mmol) was then added and the mixture was heated to reflux under vigorous stirring. A slight flow of $N_2$ was used periodically to remove CO and to maintain the presence of an inert gas in the reaction flask. The initial pale yellow solution turned bright red, and the conversion was measured by checking the characteristic infrared ν(CO) stretching bands of the starting [$Cr(CO)_6$] and of the reaction product. The reaction reached a maximum product concentration after ca. 2 d, when some decomposition began to appear. Heating was then stopped, and the solvent was evaporated under vacuum in a warm bath (45−50 °C, 2500 Pa). The resultant residue was dissolved in toluene (a few mL) and the solution was chromatographed on a 25-cm column, with SilicaGel60 as stationary phase and toluene as eluent. The excess [$Cr(CO)_6$] rapidly eluted, whilst a pale yellow band due to the remaining pyrene partially overlapped the deep red band of complex **1**. This fraction was collected and reduced to ca. 5 mL under a gentle flow of $N_2$. Crystallization under $N_2$ at 0 °C gave rise to bright red needles of pure complex **1** in a yield of ca. 45% (with respect to the starting pyrene). The crystals are stable in air for weeks and quite stable in solution, provided they are kept under anaerobic conditions.

**(b) [(Perylene)Cr(CO)$_3$] (2):** Reactants: perylene (200 mg, 0.79 mmol) and hexacarbonylchromium (1.25 g, 5.68 mmol); reaction conditions: as before; product: bulky dark purple crystals in ca. 35% yield after 4−5 d standing at −30 °C. **2** is air-stable in the solid state for several days, rather stable in anaerobic hydrocarbon solutions, and very unstable when dissolved in halogenated solvents ($CH_2Cl_2$, $CCl_4$), even under the strictest anaerobic conditions.

**(c) [(Chrysene)Cr(CO)$_3$] (3):** Reactants: chrysene (200 mg, 0.88 mmol) and [$Cr(CO)_6$] (1 g, 4.54 mmol); reaction conditions: as before; product: bright bulky red crystals (yield ca. 55%), obtained after 3−4 d standing at −30 °C; the complex is very stable on air, and quite stable in anaerobic solutions. Because **3** co-crystallizes with toluene, to avoid crystal efflorescence the crystals must be stored in the presence of toluene vapor at low temperatures.

**(d) [(1,2-Benzanthracene)Cr(CO)$_3$] (4):** Reactants: 1,2-benzanthracene (150 mg, 0.66 mmol) and $Cr(CO)_6$ (1 g, 4.54 mmol); reaction conditions: as before; product: bright red needles (yield ca. 65%), obtained after dissolution of **4** in benzene and 15 d of standing at 7 °C. The complex is stable in air in the solid state, and quite stable in solution under anaerobic conditions.

**X-ray Structure Analysis:** X-ray data for complexes **1**−**4** were collected at room temperature, with a Siemens P4 diffractometer, equipped with an APEX CCD detector 6 cm from the crystal. Graphite-monochromatized Mo-$K_\alpha$ radiation was used with a generator working at 50 kV and 40 mA for **1** and **2** and 35 mA for **3** and **4**. To avoid the loss of solvent (toluene), the crystal of **3** was mounted in a Lindemann glass capillary, with a drop of mother solution inside. Unit cell parameters were obtained by least-squares refinement of 46 (**1**), 31 (**2**), 60 (**3**) and 60 (**4**) reflections in the 2θ range 10−45°. For data collection and refinement, the package of Bruker AXS programs (SMART, SAINT, SADABS, SHELXTL)[71] was used. Owing to the small dimensions and low diffraction power of some crystals, the exposure time of the frames for data collections was 30 (**1** and **2**), 20 (**3**) and 10 s (**4**). The reflections were collected using the ω-scan technique ($\Delta\omega$ = 0.3°) and the intensities were corrected for absorption with the multi-scan method (SADABS) for **1**, **3** and **4**, while for **2** the numerical crystal faces method was applied (XPREP). In complex **3** a disordered molecule of toluene, lying on the inversion centre, was located. The non-hydrogen atoms were anisotropically refined. High thermal parameters were found for the four complexes. Hydrogen atoms in calculated positions were refined riding on the corresponding carbon atom. Crystal data and refinement parameters are

  

Table 4. Crystal and structure refinement data for complexes **1**−**4**

| Compound | **1** | **2** | **3** | **4** |
|---|---|---|---|---|
| Empirical formula | $C_{19}H_{10}CrO_3$ | $C_{23}H_{12}CrO_3$ | $C_{24.5}H_{15.5}CrO_3$ | $C_{21}H_{12}CrO_3$ |
| Formula mass | 338.27 | 388.33 | 409.87 | 264.31 |
| Temperature [K] | 294(2) | 293(2) | 294(2) | 298(2) |
| Wavelength [Å] | 0.71073 | 0.71073 | 0.71073 | 0.71073 |
| Crystal system, space group | monoclinic, $P2_1/n$ | monoclinic, $C2/c$ | triclinic, $P\bar{1}$ | orthorhombic, *Pbca* |
| *a* [Å] | 12.8686(17) | 17.818(2) | 9.990(9) | 12.8320(10) |
| *b* [Å] | 7.2639(9) | 12.955(1) | 10.172(9) | 12.1077(10) |
| *c* [Å] | 15.0804(18) | 14.632(2) | 10.391(8) | 20.2644(16) |
| α [°] | 90 | 90 | 94.033(15). | 90 |
| β [°] | 95.837 | 101.073(2) | 104.864(14) | 90 |
| γ [°] | 90 | 90 | 108.807(14) | 90 |
| Volume [$Å^{-3}$] | 1402.3(3) | 3314.5(6) | 952.5(14) | 3148.4(4) |
| *Z*, calcd. density [$g/cm^{-3}$] | 4, 1.602 | 8, 1.556 | 2, 1.429 | 8, 1.537 |
| μ [$mm^{-1}$] | 0.828 | 0.712 $mm^{-1}$ | 0.623 | 0.744 |
| *F*(000) | 688 | 1584 | 421 | 1488 |
| Crystal size [mm] | 0.040 × 0.08 × 0.28 | 0.02 × 0.16 × 0.38 | 0.30 × 0.32 × 0.44 | 0.18 × 0.34 × 0.36 |
| Color, shape | dark red, prism | black, prism | red, prism | red, lamina |
| θ range for data collected [°] | 2.72 to 28.31 | 1.96 to 28.31 | 2.06 to 28.37 | 2.01 to 28.35 |
| Limiting indices | $-14 \le h \le 16$<br>$-9 \le k \le 8$<br>$-20 \le l \le 20$ | $-23 \le h \le 23$<br>$-14 \le k \le 17$,<br>$-19 \le l \le 19$ | $-12 \le h \le 13$<br>$-13 \le k \le 12$<br>$-13 \le l \le 13$ | $-16 \le h \le 17$<br>$-16 \le k \le 15$<br>$-26 \le l \le 25$ |
| Reflections collected/unique | 9792/3361 [*R*(int) = 0.0471] | 11753/3879 [*R*(int) = 0.0474] | 6914/4360 [*R*(int) = 0.0284] | 21032/3761 [*R*(int) = 0.0371] |
| Refinement method | Full-matrix least squares on $F^2$ | Full-matrix least squares on $F^2$ | Full-matrix least squares on $F^2$ | Full-matrix least squares on $F^2$ |
| Data/restraints/parameters | 3361/0/208 | 3879/0/244 | 4360/1/262 | 3761/0/221 |
| Goodness-of-fit on $F^2$ | 0.644 | 0.734 | 0.828 | 0.880 |
| Final *R* indices[a] [$I > 2\sigma(I)$] | *R*1 = 0.0361, *wR*2 = 0.0578 | *R*1 = 0.0402, *wR*2 = 0.0828 | *R*1 = 0.0445, *wR*2 = 0.0940 | *R*1 = 0.0375, *wR*2 = 0.0907 |
| *R* indices (all data) | *R*1 = 0.0975, *wR*2 = 0.0622 | *R*1 = 0.0812, *wR*2 = 0.0870 | *R*1 = 0.0698, *wR*2 = 0.0992 $eÅ^{-3}$ | *R*1 = 0.0643, *wR*2 = 0.0951 |
| Largest diff. peak/hole [$e·Å^{-3}$] | 0.368/−0.215 | 0.426/−0.232 | 0.305/−0.233 | 0.488/−0.380 |

[a] $R1 = \Sigma||F_o| - |F_c||/\Sigma|F_o|$ for "observed" reflections having $F_o^2 > 2\sigma(F_o^2)$. $wR2 = [\Sigma(wF_o^2 - F_c^2)^2/\Sigma w(F_o^2)^2]^{1/2}$. Goodness-of-fit = $[\Sigma w(F_o^2 - F_c^2)^2/(\text{no. of unique reflections} - \text{no. of parameters})]^{1/2}$.

reported in Table 4. CCDC-211599 to·-211602 contain the supplementary crystallographic data for this paper. These data can be obtained free of charge at www.ccdc.cam.ac.uk/conts/retrieving.html [or from the Cambridge Crystallographic Data Centre, 12 Union Road, Cambridge CB2 1EZ, UK; Fax: (internat.) + 44-1223/336-033; E-mail: deposit@ccdc.cam.ac.uk].

**Vibrational Analysis:** Infrared spectroscopy measurements were recorded in solutions of dried *n*-heptane and toluene or in KBr pellets with a Bruker FTIR Equinox 55 spectrophotometer (resolution 2 $cm^{-1}$). Raman measurements were performed on crystal samples, sealed in a glass capillary under Ar, with a Bruker RFS 100 spectrophotometer (resolution 4 $cm^{-1}$) equipped with a 1.064 nm Nd:YAG laser, irradiating the samples with an average power set in the range 30−45 mW. Ab initio calculations of the free PAH were performed by employing the DFT B3LYP method with the Gaussian 98[72] package on a personal computer. We used a 6-31G** basis set and the vibrational frequencies and intensities and normal coordinates were calculated at the respective optimised structure. For the 1700−100 $cm^{-1}$ region we employed a scaling factor of 0.9614. Normal coordinates were visualized with the Moldraw package.[73] The accordance between the scaled DFT and experimental frequencies was very good, and the intensity vibrational pattern was well fitted.

**NMR Spectra:** All NMR data were acquired with a Jeol EX 400 operating at 399.6 MHz. One-dimensional $^1H$ spectra were recorded in deuterated benzene and toluene solutions, with 32 K data points and a sweep width of 5827 Hz giving a digital resolution of 0.35 Hz; 64 accumulations were acquired with an acquisition time of 2.8 s. Two-dimensional $^1H$-$^1H$ spectra were acquired with a spectral width of 5500 Hz, 512 $t_1$ points, 2 K data points in $t_2$ and 32 transients for each $t_2$ points. Chemical shifts were referenced to tetramethylsilane (TMS).

## Acknowledgments

We are indebted to the Italian MIUR (Ministero dell'Istruzione, dell'Università e della Ricerca) for their support (FIRB) of this research.

[1] J. Szczepanski, M. Vala, *Astrophys. J.* **1993**, *414*, 646−655.
[2] T. Watube, T. Ishizuka, M. Isobe, N. Ozawa, *Science.* **1982**, *215*, 403−405.
[3] J. A. Morley, N. F. Woolsey, *J. Org. Chem.* **1992**, *57*, 6487−6495.
[4] R. G. Harvey, *Polyciclic Hydrocarbons and Carcinogenesis*, American Chemical Society, Washington, DC, **1985**, pp. 406.
[5] A. I. Kitaigorodsky, *Molecular crystals and molecules*, Academic Press, New York, **1973**, pp. 38−48.
[6] V. Balzani, S. Campagna, G. Denti, A. Juris, S. Serroni, A. Venturi, *Acc. Chem. Res.* **1998**, *31*, 26−34.
[7] F. Casellato, C. Vecchi, A. Girelli, P. G. Farrell, *Thermochim. Acta* **1975**, *13*, 37−45.
[8] I. Ikemoto, H. Kuroda, *Acta Crystallogr., Sect. B* **1968**, *24*, 383−387.
[9] P. J. Munnoch, J. D. Wright, *J. Chem. Soc., Perkin Trans. 2* **1974**, 1397−1400.
[10] J. S. Lee, K. C. Huang, W. J. Wang, J. L. Wang, *Synth. Met.* **1995**, *70*, 1227−1228.
[11] R. Atencio, K. V. Domasevitch, M. J. Zaworotko, *Crystal Engineer.* **2000**, *3*, 63−69.

  

[12] D. E. Eaton, A. G. Anderson, J. C. Calabrese, W. Tam, Y. Wang, *J. Am. Chem. Soc.* **1987**, *109*, 1886−1888.
[13] R. L. De, J. Von Seyerl, L. Zsolnai, G. Huttner, *J. Organomet. Chem.* **1979**, *175*, 185−191.
[14] D. Braga, F. Grepioni, K. Biradha, V. R. Pedireddi, G. R. Desiraju, *J. Am. Chem. Soc.* **1995**, *117*, 3156−3166.
[15] N. J. Long, *Angew. Chem. Int. Ed. Engl.* **1995**, *34*, 21−38.
[16] D. Braga, F. Grepioni, G. R. Desiraju, *Chem. Rev.* **1998**, *98*, 1375−1405.
[17] B. Deubzer, E. O. Fischer, H. P. Fritz, C. G. Kreiter, N. Kriebitzsch, H. D. Simmons, B. R. Willeford, Jr., *Chem. Ber.* **1967**, *100*, 3084−3096.
[18] E. O. Fischer, K. Oefele, *Chem. Ber.* **1957**, *90*, 2532−2535.
[19] G. Natta, R. Ercoli, F. Calderazzo, *Chem. Ind. (Milan)* **1958**, *40*, 287−289.
[20] G. Natta, R. Ercoli, F. Calderazzo, *Chem. Ind. (Milan)* **1958**, *40*, 1003−1007.
[21] A. D. Hunter, L. Shilliday, W. S. Furey, M. J. Zaworotko, *Organometallics* **1992**, *11*, 1550−1560.
[22] [22a] A. Solladié-Cavallo, *Polyhedron* **1985**, *4*, 901−927. [22b] W. E. Silverthorn, *Adv. Organomet. Chem.* **1975**, *13*, 47−137. [22c] C. V. Senoff, *Coord. Chem. Rev.* **1980**, *32*, 11−191.
[23] V. Kunz, W. Novacki, *Helv. Chim. Acta* **1967**, *50*, 1052−1059.
[24] F. Hanic, O. S. Mills, *J. Organomet. Chem.* **1968**, *11*, 151−158.
[25] [25a] K. W. Muir, G. Ferguson, G. A. Sim, *J. Chem. Soc., B.* **1968**, 467−471. [25b] J. M. Guss, R. Mason, *J. Chem. Soc., Dalton Trans.* **1973**, 1834−1838.
[26] R. D. Rogers, J. L. Atwood, T. A. Albright, W. A. Lee, M. D. Rausch, *Organometallics* **1984**, *3*, 263−270.
[27] Cambridge Structural Database (CSD), Cambridge, UK, **2002**.
[28] I. Chavez, A. Cisternas, M. Otero, E. Roman, U. Muller, *Z. Naturforsch., Teil B* **1990**, *45*, 658−666.
[29] L. C. Porter, J. R. Polam, J. Mahmoud, *Organometallics* **1994**, *13*, 2092−2096.
[30] L. C. Porter, J. R. Polam, S. Bodige, *Inorg. Chem.* **1995**, *34*, 998−1001.
[31] M. Crocker, M. Green, J. A. K. Howard, N. C. Norman, D. M. Thomas, *J. Chem. Soc., Dalton Trans.* **1990**, 2299−2301.
[32] R. G. Swisher, E. Sinn, R. N. Grimes, *Organometallics* **1985**, *4*, 896−901.
[33] H. Kubo, M. Hirano, S. Komiya, *J. Organomet. Chem.* **1998**, *556*, 89−100.
[34] N. P. Do Thi, S. Spichiger, P. Paglia, G. Bernardinelli, E. P. Kündig, P. L. Timms, *Helv. Chim. Acta* **1992**, *75*, 2593−2607.
[35] J. K. Seaburg, P. J. Fischer, V. G. Young, J. E. Ellis, *Angew. Chem. Int. Ed.* **1998**, *37*, 155−158.
[36] B. P. Byers, M. B. Hall, *Inorg. Chem.* **1987**, *26*, 2186−2188.
[37] S. M. Hubig, S. V. Lindeman, J. K. Kochi, *Coord. Chem. Rev.* **2000**, *200−202*, 831−873.
[38] M. Sodeoka, H. Yamada, M. Shibasaki, *J. Am. Chem. Soc.* **1990**, *112*, 4906−4911.
[39] R. H. Mitchell, Y. Chen, *Tetrahedron Lett.* **1996**, *37*, 6665−6668.
[40] R. H. Mitchell, Y. Chen, N. Khalifa, P. Zhou, *J. Am. Chem. Soc.* **1998**, *120*, 1785−1794.
[41] R. H. Mitchell, Z. Brkic, D. J. Berg, T. M. Barclay, *J. Am. Chem. Soc.* **2002**, *124*, 11983−11988.
[42] For example e.s.d.s of 0.002−0.003 Å were obtained by neutron data at 78 K on [$C_6H_6Cr(CO)_3$]: B. Rees, P. Coppens, *Acta Crystallogr., Sect. B* **1973**, *29*, 2516−2528.
[43] J. Y. Sailard, D. Grandjean, P. LeMaux, G. Jaouen, *New J. Chem.* **1981**, *5*, 153−160.
[44] P. G. Gassman, P. A. Deck, *Organometallics* **1994**, *13*, 1934−1939.
[45] B. Rees, A. Mitschler, *J. Am. Chem. Soc.* **1976**, *98*, 7918−7924.
[46] A. D. Hunter, V. Mozol, S. D. Tsai, *Organometallics* **1992**, *11*, 2251−2262.
[47] M. Randić, *Chem. Rev.* **2003**, *103*, 3449−3605.
[48] A. Stanger, R. Boese, N. Askenazi, P. Stellberg, *J. Organomet. Chem.* **1997**, *542*, 19−24.
[49] M. Nambu, D. L. Mohler, K. Hardcastle, K. K. Baldridge, J. S. Siegelpp, *J. Am. Chem. Soc.* **1993**, *115*, 6138−6142.
[50] E. L. Muetterties, J. R. Bleeke, E. J. Wucherer, T. A. Albright, *Chem. Rev.* **1982**, *82*, 499−525.
[51] T. A. Albright, P. Hofmann, R. Hoffmann, C. P. Lillya, P. A. Dobosh, *J. Am. Chem. Soc.* **1983**, *10*, 3396−3411.
[52] E. Diana, R. Rossetti, P. L. Stanghellini, S. F. A. Kettle, *Inorg. Chem.* **1997**, *36*, 382−391.
[53] S. R. Langhoff, *J. Phys. Chem.* **1996**, *100*, 2819−2841.
[54] A. Berces, T. Ziegler, *J. Phys. Chem.* **1994**, *98*, 13233−13242.
[55] J. Muller, T. Akhnoukh, P. E. Gaede, A. Guo, P. Moran, K. Qiao, *J. Organomet. Chem.* **1997**, *541*, 207−217.
[56] L. Schäfer, J. Southern, S. J. Cyvin, *Spectrochim. Acta* **1971**, *27A*, 1083−1090.
[57] Table 2SI of the Supporting Information lists the most important infrared and Raman bands of the complexes and the proposed assignment.
[58] For example, for complex **1**, $\Delta\gamma$(CH) is 18 cm$^{-1}$ in solid-state spectra and ca. 0 cm$^{-1}$ in $CS_2$ solution.
[59] D. M. Hudgins, L. J. Allamandola, *J. Phys. Chem. A* **1997**, *101*, 3472−3477.
[60] J. Price, T. S. Sorensen, *Can. J. Chem.* **1968**, *468*, 515−522.
[61] R. V. Emanuel, E. W. Randail, *J. Chem. Soc., A* **1969**, 3002−3006.
[62] M. J. McGlinchey, S. T. Tan, *Can. J. Chem.* **1974**, *52*, 2439−2443.
[63] M. J. McGlinchey, J. L. Fletcher, *Can. J. Chem.* **1975**, *53*, 1525−1529.
[64] E. P. Kündig, V. Desorby, C. Griver, B. Rudolf, S. Spichiger, *Organometallics* **1987**, *6*, 1173−1180.
[65] Y. F. Oprunenko, S. G. Malugina, Y. A. Ustynyuk, N. A. Ustynyuk, D. N. Kravtsov, *J. Organomet. Chem.* **1988**, *338*, 357−368.
[66] S. D. Cunningham, K. Oefele, B. R. Willeford, *J. Am. Chem. Soc.* **1983**, *105*, 3724−3725.
[67] Y. F. Oprunenko, N. G. Akhmedov, D. N. Laikov, S. G. Malyugina, V. I. Mstislavsky, A. R. Vitaly, Y. A. Ustynyuk, N. A. Ustynyuk, *J. Organomet. Chem.* **1999**, *583*, 136−145.
[68] B. Deubzer, H. P. Fritz, C. G. Kreiter, K. Öfele, *J. Organomet Chem.* **1967**, *7*, 289−299.
[69] K. M. Nicholas, R. C. Kerber, E. I. Stiefel, *Inorg. Chem.* **1971**, *10*, 1519−1521.
[70] P. Bergamini, E. Costa, S. Sostero, A. G. Orpen, P. G. Pringle, *Organometallics* **1991**, *10*, 2989−2990.
[71] Bruker AXS, Inc., Madison, Wisconsin, **2003**.
[72] M. J. Frisch, G. W. Trucks, H. B. Schlegel, G. E. Scuseria, M. A. Robb, J. R. Cheeseman, V. G. Zakrzewski, J. A. Montgomery, Jr., R. E. Stratmann, J. C. Burant, S. Dapprich, J. M. Millam, A. D. Daniels, K. N. Kudin, M. C. Strain, O. Farkas, J. Tomasi, V. Barone, M. Cossi, R. Cammi, B. Mennucci, C. Pomelli, C. Adamo, S. Clifford, J. Ochterski, G. A. Petersson, P. Y. Ayala, Q. Cui, K. Morokuma, D. K. Malick, A. D. Rabuck, K. Raghavachari, J. B. Foresman, J. Cioslowski, J. V. Ortiz, A. G. Baboul, B. B. Stefanov, G. Liu, A. Liashenko, P. Piskorz, I. Komaromi, R. Gomperts, R. L. Martin, D. J. Fox, T. Keith, M. A. Al-Laham, C. Y. Peng, A. Nanayakkara, M. Challacombe, P. M. W. Gill, B. Johnson, W. Chen, M. W. Wong, J. L. Andres, C. Gonzalez, M. Head-Gordon, E. S. Replogle, J. A. Pople, *Gaussian 98, Revision A.9*, Gaussian, Inc., Pittsburgh PA, **1998**.
[73] P. Ugliengo, D. Viterbo, G. Chiari, *Z. Kristallogr.* **1993**, *207*, 9−23.


Received June 14, 2003
Early View Article
Published Online February 17, 2004

  